JOURNAL OF VIROLOGY, Dec. 2008, p. 12510–12519 Vol. 82, No. 24
0022-538X/08/$08.00+0 doi:10.1128/JVI.00458-08

Neuroadapted Yellow Fever Virus Strain 17D: a Charged Locus in Domain III of the E Protein Governs Heparin Binding Activity and Neuroinvasiveness in the SCID Mouse Model[▽]

Janice Nickells, Maria Cannella, Deborah A. Droll, Yan Liang, William S. M. Wold, and Thomas J. Chambers*

Department of Molecular Microbiology and Immunology, Doisy Research Center, St. Louis University School of Medicine, 1100 South Grand Boulevard, St. Louis, Missouri 63104

Received 2 March 2008/Accepted 25 September 2008

A molecular clone of yellow fever virus (YFV) strain 17D was used to identify critical determinants of mouse neuroinvasiveness previously localized to domain III of the neuroadapted SPYF-MN virus envelope protein. Three candidate virulence substitutions (305F→V, 326K→E, and 380R→T) were individually evaluated for their roles in this phenotype in a SCID mouse model. The virus containing a glutamic acid residue at position 326 of the envelope protein (326E) caused rapidly lethal encephalitis, with a mortality rate and average survival time resembling those of the parental SPYF-MN virus. Determinants at positions 380 (380T) and 305 (305V) did not independently affect neuroinvasiveness. Testing a panel of viruses with various amino acid substitutions at position 326 revealed that attenuation of neuroinvasiveness required a positively charged residue (lysine or arginine) at this position. Molecular-modeling studies suggest that residues 326 and 380 contribute to charge clusters on the lateral surface of domain III that constitute putative heparin binding sites, as confirmed by studies of heparin inhibition of plaque formation. The neuroinvasiveness of YFVs in the SCID model correlated inversely with sensitivity to heparin. These findings establish that residue 326 in domain III of the E protein is a critical determinant of YFV neuroinvasiveness in the SCID mouse model. Together with modeling of domain III from virulent YFV strains, the data suggest that heparin binding activity involving lysine at position 326 may be a modulator of YFV virulence phenotypes.

Yellow fever virus (YFV), the prototype member of the genus *Flavivirus*, is inherently neurotropic for rodent and primate hosts, causing acute encephalitis after virus entry into the central nervous system (4, 26). This syndrome is sometimes observed as a complication after vaccination of humans with the YFV 17D strain (9). Strains of YFV are known to differ in their neurovirulence potentials (2, 8, 18, 31, 32), and this property can be enhanced by serial passage of the virus in brain tissue (7, 25, 34, 36). Mutations in numerous regions of the viral genome have been identified in such neuroadapted viruses, although the viral E envelope protein is believed to contain the most important determinants of this virulence (3, 33). Mutations in the flavivirus E protein are likely to contribute enhanced virulence through effects on virus entry into host cells and spread to critical target tissues (11, 20, 22, 23, 27, 28, 31, 32), although the exact mechanisms involved in this process have not been defined.

In a previous study, the genetic determinants of neuroinvasiveness of a neuroadapted strain of YFV 17D (SPYF-MN) in SCID mice were localized to the viral E protein (29). Viruses containing either the entire E protein or only domain III of the parental neuroinvasive SPYF-MN virus in the background of the nonneuroadapted YF5.2iv virus (YFV 17D molecular clone) were found to be neuroinvasive for young SCID mice. A total of three nucleotide substitutions encoding three amino acid substitutions in domain III of the E protein (E305-V, E326-E, and E380-T) were thus implicated as determinants of this neuroinvasiveness. In the current study, the objective was to further characterize the contributions of these three substitutions to the neuroinvasive phenotype and to investigate the molecular requirements at any of the three positions that were identified as virulence determinants. This was accomplished by constructing and testing viruses containing the single neuroadaptive substitutions at positions 305, 326, and 380, as well as a panel of viruses containing amino acid substitutions at position 326, which was identified as a critical virulence determinant.

MATERIALS AND METHODS

Cells and viruses. Vero and BHK cells were grown at 37°C in alpha minimal essential medium (alpha-MEM) supplemented with 10% fetal bovine serum. The neuroadapted SPYF-MN virus clone, the SPYF-H3 virus (previously referred to as SPYF-E_{III}), and YF5.2iv virus generated from a YFV 17D molecular clone have been described previously (3, 29). Dengue 2 virus, used for heparin binding experiments, was described previously (5). Plaque assays for the quantitation of infectious virus were done in Vero cells under an agarose overlay as previously described (37). In later experiments, plaque assays were done using the addition of carboxymethyl-cellulose overlay medium (1% [wt/vol] carboxymethyl-cellulose [Sigma; C-4888] in alpha-MEM) containing 4 to 5% fetal bovine serum and 100 U of penicillin-streptomycin. The plates were incubated for 5 to 6 days at 37°C and 5% CO_2 to allow plaque formation, which was then visualized by adding 1.0 ml of crystal violet (0.13% [wt/vol] crystal violet, 5% ethanol, 10% formaldehyde) directly to the carboxymethyl-cellulose overlay and incubating the plates at room temperature for 1 h. The plates were rinsed with water to remove the stain, and the plaques were then counted. Direct comparison of the two

* Corresponding author. Mailing address: Department of Molecular Microbiology and Immunology, Doisy Research Center, St. Louis University School of Medicine, 1100 South Grand Blvd., St. Louis, MO 63104. Phone: (314) 977-8711. Fax: (314) 977-8717. E-mail: thomas_chambers2@merck.com.

▽ Published ahead of print on 8 October 2008.

methods of plaque assay revealed very similar titers, but the plaque sizes of individual viruses differed in some cases. For experiments involving inoculation of mice, viruses were diluted in alpha-MEM plus 10% fetal bovine serum.

Mouse experiments. SCID/ICR mice were obtained from Taconic Farms, Germantown, NY, and used in accordance with the guidelines of the Institutional Animal Care and Use Committee. Mice between 4 and 5 weeks of age were used in studies of neuroinvasiveness. The mice were housed in microisolator units and handled under sterile conditions during all procedures. Tests of neuroinvasiveness were conducted by inoculation by the intraperitoneal (i.p.) route, with mice being observed for signs of illness and euthanized at the onset of neurologic disease (either encephalitis or hind-limb paralysis). Experiments to measure the virus content in mouse tissues were done by recovering tissue samples by dissection after perfusion with phosphate-buffered saline (PBS) at 4°C. Samples were stored at −70°C, thawed, and homogenized as 10% suspensions in PBS plus 10% fetal bovine serum using a Dounce homogenizer. Virus quantitation was done by performing plaque assays of diluted samples on Vero cell monolayers under 1.0% ME agarose (SeaKem) in alpha-MEM plus 5% fetal bovine serum. Plaques were visualized by staining them with 0.05% neutral red in PBS after 6 to 7 days of incubation, followed by fixation in 10% formalin and counterstaining with crystal violet.

Construction of mutant viruses. The YF5.2iv molecular clone was used for the construction of mutant viruses. This clone is based on a two-plasmid system for assembly of DNA templates for transcription of infectious YFV RNA (30). pYF5′3′IV contains YFV nucleotide sequences from nucleotide (nt) 1 to 2271 and nt 8275 to 10862 (YFV numbering) downstream of an SP6 promoter, and pYFM5.2 contains the YFV sequence from nt 1363 to 8704.

pYFM5.2 harboring SPYF-MN nucleotide substitutions at positions 1886, 1949, 2112, and 2431, described previously (29), was used as starting material for isolation of the SPYF amino acid substitutions into separate YFVs as follows. The 2112 and 2431 substitutions, encoding the E protein substitution R to T at position 380 and a silent substitution at position 486, respectively, were isolated in a fragment from nt 1959 to 5459 (YFV genome numbering) following digestion with Sse8387I and NheI. pYFM5.2, harboring only the parental YF5.2iv sequence, was similarly digested, and the fragment containing nt 5459 to 1959 was recovered. These fragments were ligated to produce the pYFM5.2 plasmid harboring the 2112 and 2431 nucleotide substitutions. The preparation of YFM5.2 plasmids containing a nucleotide substitution at either nt 1886 or nt 1949, encoding the amino acid substitutions F to V at position 305 and K to E at position 326, respectively, was performed in three steps. First, pYFM5.2 containing the 1886 and 1949 substitutions was digested with BamHI and the fragment containing both substitutions was self-ligated to produce pYFM5.2-del-BamHI. pYFM5.2 containing only the YFM5.2 sequence was treated in the same manner. Second, both pYFM5.2-del BamHI plasmids were digested with NcoI, and reciprocal ligations were performed exchanging the fragments containing nt 1619 to 1915 and 1915 to 1619. Third, the deletions between the BamHI restriction sites were replaced with fragments prepared by digestion of both single mutant BamHI deletion plasmids and the pYFM5.2 plasmid containing only the 5.2iv sequence with Sse8387I and XbaI. The pYFM5.2-derived fragment between nt 1959 and 8728 (within the vector) was ligated to the single mutant fragments to reconstruct the complete pYFM5.2 plasmids containing either the F305 to V or 326K to E substitution.

Nucleotide substitutions in pYFM5.2 to introduce amino acid substitutions at position 326 were made using the QuickChange II Site-Directed Mutagenesis Kit (Strategene) following the manufacturer's recommendations. The sequence of the forward mutagenesis primer corresponding to nt 1923 to 1957 (YF5.2iv genome numbering), with the codon for position 326 (lysine, as in YF5.2iv) underlined, was as follows: 5′-CT GTT GTG ATG CAG GTG AAA GTG TCA AAA GGA GCC-3′. The reverse primers had the complementary sequences. Thermal cycling to amplify the mutant strands was performed under the following conditions: initial denaturation at 95°C for 1 min, followed by cycles of 95°C for 50 s, 60°C for 50 s, and 68°C for 10 min for a total of 18 cycles, followed by 7 min at 68°C. The PCR products were incubated with DpnI to degrade the template strands, and the mutant plasmids were recovered from 0.8% low melting temperature (LMT) agarose gels and purified using a Wizard PCR product purification kit (Promega). The plasmids were then used to transform XL10-Gold ultracompetent *Escherichia coli* on LB plates containing ampicillin, and the recovered colonies were used to prepare plasmid DNA from small cultures in LB medium with ampicillin. A YF2162(−) primer (nt 1949 to 1951) was used to sequence through the site of the mutation to verify the correct plasmids.

Transcription, RNA transfection, and virus recovery. Full-length templates for synthesis of RNA transcripts were prepared as described previously (3, 29). pYF5′3′IV and pYFM5.2 derivatives were digested with NsiI and AatII, the appropriate fragments were isolated from LMT agarose gels and ligated in vitro, and the ligation product was digested with XhoI to linearize the template. RNA transcripts were then generated by runoff transcription. Vero cells were then transfected with approximately 100 ng of RNA transcript to produce infectious virus. The viruses were harvested following the appearance of cytopathic effects, typically 3 to 5 days following transfection, and virus yields were quantitated by plaque assay on Vero cells as described above. The E protein region was sequenced from PCR products from total cellular RNA recovered from infected Vero cell monolayers. For viruses giving the desired sequence, the transfection harvests were then plaque purified on Vero cells and amplified on BHK cells for two rounds of plaque purification. Total RNA from the cell monolayers from which the amplified stocks were prepared was used to verify the sequence of the E protein region prior to further experiments.

Nucleotide sequencing. All sequencing reactions for the YF5.2iv, F305V, R380T, SPYF-H3, and 326 mutant viruses were performed on PCR products generated by reverse transcriptase PCR from total cellular RNA isolated from cell culture monolayers. First-strand reactions were run using the YF2980(−) primer, together with a portion of total RNA from the infected Vero monolayer and Superscript II reverse transcriptase (Invitrogen). The mixture was incubated at 42°C for 50 min to permit first-strand synthesis and then for 15 min at 70°C to inactivate the reverse transcriptase. The RNA templates were then degraded with RNase (Invitrogen). The cDNA reaction was then used to generate a PCR product containing the complete prM-E region using the Triple Master kit (Eppendorf), following the manufacturer's protocol. The primer pair used for amplification was as follows: YF5′(+) (5′-GAGTAAATCCTGTGTGCTAATTG-3′) and YF2486-2509(−) (5′-GATACCATTTCCGCACTTGAGCTC-3′.

The specifics of the thermal cycling were as follows: 95°C for 2 min, followed by 95°C for 1 min, 50°C for 1 min, and 72°C for 1.5 min for a total of 35 cycles, followed by 72°C for 7 min. Following amplification, the PCR products were recovered from 1% LMT agarose gels and purified using the Wizard PCR purification kit (Promega). The recovered PCR products were then sequenced using the following sequencing primers for the prM-E region: YF440(+) (5′-CGCCGTTCCCATGATGTTCTGACTG-3′), YF941(+) (5′-GACGCAATGAGTCGTGATTGCCC-3′), YF2162(−) (5′-CATGGTCTGAGTGAACAACTTTCC-3′), and YF2486(−) (5′-GATACCATTTCCGCACTTGAGCTC-3′).

Virus growth curves. Viruses were inoculated onto monolayers of BHK cells in six-well costars at 37°C in triplicate at a multiplicity of infection of 0.001 PFU/cell. The media were harvested at serial intervals postinfection, followed by replacement with fresh medium. The virus yields were determined by plaque assay on Vero cells as described above and expressed as means ± standard deviations.

Heparin-Sepharose binding assay. Viruses used for heparin-Sepharose binding assays were the plaque-purified preparations used for SCID mouse neuroinvasiveness testing. A protocol was developed essentially based on that previously described by Lee et al. (15). Fifty percent (vol/vol) Sepharose/saline suspensions (heparin-Sepharose [Sigma; H6508] and protein A-Sepharose [Sigma; P2670]) were equilibrated just prior to use by centrifugation of the beads at low speed in an Eppendorf microcentrifuge and three washes in Hank's balanced salt solution and supplemented with 10 mM HEPES and 0.2% bovine serum albumin. For each virus to be tested, approximately 10^4 PFU in 100 μl of 10 mM HEPES and 0.2% bovine serum albumin was mixed with 100 μl of heparin-Sepharose or with 100 μl of protein A-Sepharose as a control. The samples were incubated for 1 h with constant rotation at 4°C. Samples were then centrifuged for 1 min at 8,000 rpm in an Eppendorf microcentrifuge, and the supernatants were removed and assayed in duplicate for virus by plaque assay on Vero cells, as described above, in duplicate wells. The percentage of virus binding to heparin was calculated using the following formula: [1 − (infectious titer of virus mixed with heparin-Sepharose/infectious titer of virus mixed with protein A-Sepharose)] × 100.

Molecular modeling. Since the structure of the YFV E protein has not been solved, a homology model for domain III of YFV was derived based on the structure of the West Nile virus (WNV) E protein, using modeling tools available from Swiss Model. The flavivirus E protein database was queried for the optimal structure to use for the model. Sequence homology of YF5.2iv and YFV French Neurotropic Vaccine (also used for modeling) was higher with respect to Japanese encephalitis virus than WNV (49.5% and 51.7% versus 48% and 47%, respectively). However WNV was selected by the modeling program on the basis of greater similarity of local and nonlocal energy environments within the protein chain and amino acid side chains, as well as compatibility based on secondary-structure predictions and other surface characteristics. Both the entire WNV E protein (accession no. 2169A) and the domain III structure (accession no. 1s6nA) were used to generate the homology models. Analysis of substitutions within domain III was done using the Swiss-PdbViewer on Swiss Model. Multiple rotamer configurations for the amino acid side chains at the positions of interest

TABLE 1. YFVs containing SPYF-MN substitutions

Virus	Domain III residues	Plaque size[a]	Heparin sensitivity[b]	Neuroinvasiveness[c]
YF5.2iv	305F; 326K; 380R	1	High	Low
305V	305V; 326K; 380R	1	High	Low
380T	305F; 326K; 380T	1–3	High	Low
326E	305F; 326E; 380R	2.5	Low	High
SPYF-H3	305V; 326E; 380T	2.5	Low	High

[a] Plaque size in Vero cells in carboxymethyl-cellulose medium (mm).
[b] Based on experiments shown in Fig. 4A.
[c] Based on experiments shown in Fig. 2.

were analyzed, and the most favorable energy predictions were used for modeling. Space-filling models and electrostatic-potential maps of domain III for each engineered mutation were generated using programs available on the Swiss Model platform.

Statistical methodology. Differences in mortality percentages and average survival times were evaluated with Fisher's exact test and the Mann-Whitney test (two-sided), respectively. Statistical analysis for heparin binding experiments was done using paired *t* testing (two sided).

RESULTS

Construction of viruses. The viruses used in these experiments were created in the background of the YF5.2iv molecular clone and are described in Tables 1 and 2. Following recovery of virus by transfection of Vero cells, the viruses were plaque purified and amplified and the sequences of the prM-E protein regions were confirmed. All viruses contained the desired engineered substitution in domain III of the E protein region, and the sequences of prM-E regions were otherwise identical to that of the YF5.2iv virus. For viruses containing amino acid substitutions at position 326 of the E protein, three attempted substitutions did not yield the correct results. For 326N, two plaque-picked variants were found to contain the reversion to 326K. For 326Y, three plaque-picked variants consistently gave a second-site substitution of 309N→K. A virus engineered to contain a deletion of residue 326 could not be recovered after two transfection attempts.

Growth efficiencies of mutant viruses in cell culture. All viruses were characterized for growth properties in BHK cells to assess whether there were any major defects in virus production that might affect assessment of their virulence properties in the SCID mouse model. Low-multiplicity infections were employed to exaggerate any differences in cell entry and spread that might be related to effects of substitutions in domain III on the function of the E protein. The results for the viruses containing the individual SPYF-specific substitutions in domain III are shown in Fig. 1A. The YF5.2iv control virus grew to a titer of 7 log PFU/ml by 84 h. The 305V and 380T viruses exhibited growth kinetics roughly similar to those of YF5.2iv and also reached a titer of 7.0 log PFU/ml at 84 h postinfection. In contrast, the SPYF-H3 and 326E viruses both exhibited decreased rates of virus production and lower maximum titers over the time interval examined in the experiment.

TABLE 2. YFVs containing substitutions at E326

Virus	Plaque size[a]	Heparin sensitivity[b]	Neuroinvasiveness[c]
YF5.2iv (326K)	1	High	Low
326R	1	High	Low
326Q	2	Low	Intermediate
326G	2.5	Low	Intermediate
326A	3	Low	High
326S	2	Low	High
326D	2.5	Low	High
326E	1–3	Low	High

[a] Plaque size on Vero cells in carboxymethyl-cellulose medium (mm).
[b] Based on experiments shown in Fig. 4B.
[c] Based on experiments shown in Fig. 3.

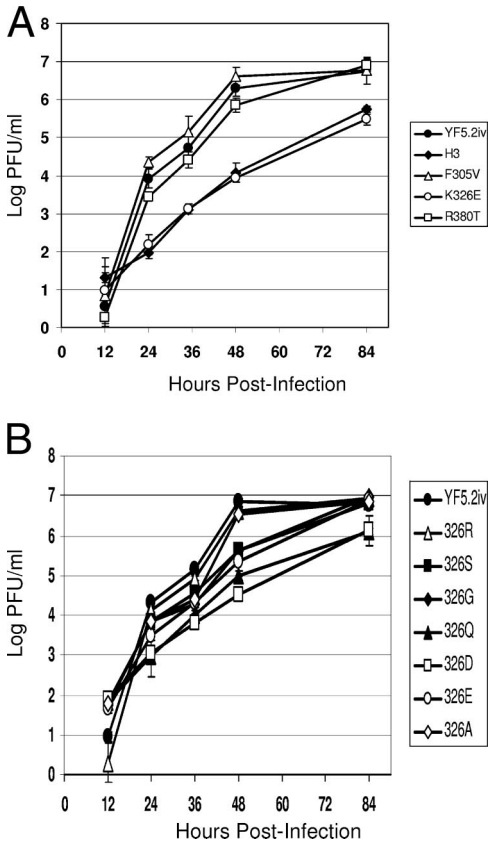

FIG. 1. Growth curves of YFVs in BHK cells. Experiments were conducted as described in Materials and Methods, using a multiplicity of infection of 0.001. The values are mean log PFU per milliliter ± 1 standard deviation for triplicate samples. (A) SPYF-H3, E326-E, E305-V, E380-T, and YF5.2iv viruses. (B) Viruses containing substitutions at position 326.

Virus containing amino acid substitutions at position 326 of the E protein were also studied for growth efficiency in BHK cells, as shown in Fig. 1B. All of the mutant viruses except 326A exhibited a delay in virus production over the initial 48 h compared to the YF5.2iv and 326R viruses. Titers for all mutants except 326Q and 326D reached levels at 84 h that were equivalent to the peak titer observed for YF5.2iv and 326R. Thus, all viruses were impaired in virus production relative to YF5.2iv and 326R, with 326Q and 326D exhibiting a significant defect in this parameter and other viruses exhibiting a moderate defect.

The reduced virus yields and production rates for 326E, 326D, and other viruses with low heparin binding capacity (see "Heparin experiments" below) could reflect less efficient growth in BHK cells as a result of impaired interactions with

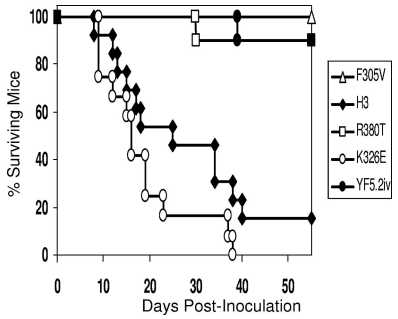

FIG. 2. Mortality data for SCID/ICR mice inoculated with YF5.2iv, 305V, 326E, 380T, or SPYF-H3 virus. Mice were inoculated with 5×10^5 PFU by the i.p. route and observed as described in Materials and Methods. Shown are mortality percentages for groups of 10 mice, except for 326E (12 mice) and SPYF-H3 (13 mice). The *P* values (two sided) for comparisons among groups based on mortality at 50 days were as follows: SPYF-H3 versus 326E, $P = 0.67$; SPYF-H3 versus 5.2 or 380T, $P = 0.0054$; SPYF-H3 versus 305V, $P = 0.0007$; YF5.2iv versus 326E, $P = 0.0019$; YF5.2iv or 380T versus 305V, $P = 0.999$; 326E versus 305V, $P = 0.0001$. The average survival time data in days (mean ± standard deviation, median) were as follows: SPYF-H3, 22.9 ± 11.2, 18; 326E, 18 ± 9.7, 15. The *P* value (two sided) for comparison of average survival times (log rank test) was 0.23.

cell surface glycosaminoglycans compared with YF5.2iv virus, with the magnitude of the effect being approximately 1.0 log unit. This factor may have some effect on dose calculations for mouse virulence testing, as explained below.

Neuroinvasiveness of 326E, 305V, and 380T viruses. Viruses containing the individual amino acid substitutions found in domain III of the SPYF envelope protein were tested for neuroinvasiveness in the SCID mouse model. The SPYF-H3 virus was used as the virulent control, since its neuroinvasiveness is similar to that of the parental neuroadapted SPYF-MN virus (3). A cutoff of 50 days was used to compare mortality percentages, as previous experiments have shown this period of time to be sufficient to distinguish the virulent SPYF-MN and SPYF-H3 from YF5.2iv virus (3, 28). Mice were inoculated with approximately 5.5 log PFU by the i.p. route. The results are shown in Fig. 2. As observed previously, mice receiving the SPYF-H3 virus exhibited high mortality (11/13 dead), and the average survival time was 23 days for the mice that died. Mice receiving the 326E mutant virus also exhibited high mortality (12/12 dead), with an average survival time of 18 days. The differencesin the mortality percentages and survival times between these two viruses were not significant. Mice receiving the 380T virus exhibited low mortality (1 of 10 mice dead at 50 days). The 305V and the YF5.2iv control viruses also exhibited low mortality (1 of 10 and 0 of 10 dead, respectively, at 56 days). The mortality rate of the 380T virus at 50 days was significantly different from those of SPYF-H3 and 326E but not from that of YF5.2iv or 305V virus. It is possible that differences in heparin binding capacities between 326E and YF5.2iv could have led to a discrepancy in the effective dose in these experiments, as the doses administered were based on plaque assay instead of mouse infectivity. However we believe this factor would not substantially alter the overall conclusions (see Discussion).

Dose range comparison of SPYF-H3 and 326E viruses. Because no significant differences in mortality rates or survival times were observed between the SPYF-H3 and 326E viruses at the dose of 5.5 log PFU, lower doses were tested to determine if any difference in neuroinvasiveness could be detected. For instance, if the neuroadaptive substitutions at positions 305 and 380 do not contribute any significant virulence effects, then there should not be differences between the degrees of neuroinvasiveness of SPYF-H3 and 326E over a range of doses. Table 3 indicates the results of two separate experiments to investigate this question. The control virus YF5.2iv exhibited no neuroinvasiveness at a dose of 5.0 log PFU. At a dose of 5 log PFU, SPYF-H3 and 326E exhibited mortality rates that were similar to those shown in Fig. 2. At a dose of 4 log PFU, the mortality rates and average survival times for SPYF-H3 and 326E were also similar. At a dose of 3 log PFU, the mortality percentages were 14/15 and 10/15, respectively, but the difference was not significant. The average survival time was slightly longer for 326E at the 3-log PFU dose. In a separate experiment, YF5.2iv exhibited low neuroinvasiveness at a dose of 5.7 log PFU. SPYF-H3 again exhibited high neuroinvasiveness at 3.0 log PFU, but at 2.0 log PFU, mortality was 0% at 60 days. For H3, high neuroinvasiveness was detected at 4.8 and 2.7 log PFU, but not at 1.6 log PFU.

Virus burdens in tissues of mice. In previous experiments, the SPYF-MN and SPYF-H3 viruses were shown to cause a systemic infection in SCID mice, which developed fatal encephalitis characterized by moderate levels of viremia, moderate virus burdens in peripheral tissues, and brain titers in excess of 7 log PFU/gram (3, 29). To determine if the 326E virus exhibited a similar pattern of infection, virus burdens were compared to those in mice infected with SPYF-H3 and YF5.2iv viruses, as shown in Table 4. Mice were subjected to i.p. inoculation with a dose of 5.5 log PFU, followed by harvest of tissues when signs of neurologic disease occurred (either hind limb paralysis or overt encephalitis). For mice inoculated with SPYF-H3, these signs were observed between days 8 and 22 (mean, day 15) postinfection, and for mice inoculated with

TABLE 3. Dose Range analysis of SPYF-H3 and 326E viruses[a]

Virus	Dose (log PFU)	Mortality	Survival time (days) [mean (SD); median]
YF5.2iv	5.0	0/10	NA[h]
SPYF-H3	5.0	15/15[b]	19.8 (7.2); 18[e]
SPYF-H3	4.0	15/15[c]	20.6 (5.3); 20[f]
SPYF-H3	3.0	14/15[d]	29.6 (5.5); 31[g]
326E	5.0	15/15 [b]	23.4 (19.6); 25[e]
326E	4.0	14/15[c]	23.3 (5.9); 22[f]
326E	3.0	10/15[d]	19.6 (6.1); 17[g]
YF5.2iv	5.7	2/8	37.5 (0.5); 37.5
SPYF-H3	3.0	6/8	34.5 (9.2); 36
SPYF-H3	2.0	0/8	NA
326E	4.8	7/8	16.75 (2.2); 16.5
326E	2.7	7/8	25 (7.1); 22
326E	1.6	0/8	NA

[a] Viruses were tested by i.p inoculation in 5-week-old SCID/ICR mice.
[b] $P = 1.0$.
[c] $P = 1.0$.
[d] $P = 0.17$.
[e] $P = 0.787$ (two sided; log rank test).
[f] $P = 0.183$ (two sided; log rank test).
[g] $P = 0.043$ (two sided; log rank test).
[h] NA, not applicable.

TABLE 4. Tissue burdens of infectious virus

Tissue	Burden[a]		
	YF5.2iv[b]	SPYF-H3	326E
Peritoneum	0/5	0/7	7/7; 2.15 ± 1.95
Spleen	2/5; 1.17 ± 0.23	3/6; 1.3 ± 0.14	0/7
Muscle	0/5	4/7; 1.86 ± 0.51	0/6
Heart	2/5; 0.95 ± 0.36	1/7; 0.7	4/6; 0.85 ± 0.07
Lung	0/5	2/7; 1.14 ± 0.13	0/7
Kidney	0/5	2/7; 1.66 ± 0.58	0/6
Adrenal	0/5	1/3; 3.3	1/3; 2.0
Brain	0/3	4/4; 8.56 ± 0.32	4/4; 7.94 ± 0.03

[a] Values indicate the number of samples positive/number of samples tested and are reported as log PFU/g (mean ± standard deviation).
[b] YF5.2iv-inoculated mice were harvested as matched controls for mice from the SPYF H3 or 326E group, even though they did not manifest signs of disease.

326E virus, between days 8 and 20 (mean, day 13). For the YF5.2iv control virus, no mice exhibited any signs of illness over this interval, and samples were harvested as matched controls at the same time that samples were taken for either the SPYF-H3 or 326E group. SPYF-H3 virus was detectable in the greatest number of peripheral organs (spleen, muscle, heart, lung, and kidney), whereas the 326E virus was consistently detected only in the peritoneum and heart. YF5.2iv virus was detected only in the heart and spleen of one mouse and either the heart or spleen of two additional mice. For both SPYF-H3 and 326E, high titers of virus were detected in the brain (8.6 log PFU/g and 7.9 log PFU/g, respectively) and moderate titers were detected in some of the adrenal glands. YF5.2iv virus was not detected in these organs. The plaque sizes of the viruses recovered from brains and peripheral tissues of mice infected with SPYF-H3 and 326E viruses, and from peripheral tissues of mice infected with YF5.2iv viruses, were similar to those of the viruses used for inoculation, suggesting no reversion over the course of the experiment to measure tissue burdens. As mentioned earlier for virus production experiments in BHK cells, differences in heparin binding activities between YF5.2iv and either SPYF-H3 or 326E could have affected the levels of virus quantitation in peripheral tissues based on greater tissue uptake of YF5.2iv virus as a result of more efficient interaction with cell surface glycosaminoglycans.

Mutagenesis of position E326. To further investigate the molecular basis for the high neuroinvasiveness exhibited by the 326E virus, a panel of viruses containing a range of different amino acid substitutions at position E326 were engineered and tested in the SCID mouse model. The primary objective of these experiments was to determine if the negatively charged glutamic acid residue at position 326 was an obligatory requirement for the neuroinvasiveness of YFV in this model. The viruses are indicated in Table 2, and the neuroinvasiveness of the viruses is shown in Fig. 3. As shown in Fig. 2, the 326E virus caused rapid mortality in all mice, with an average survival time of 18 days. The 326D virus was also highly neuroinvasive, with 80% mortality within 50 days. The 326A and 326S viruses also exhibited high neuroinvasiveness, with day 50 mortality not significantly different from that of 326E or 326D. The 325G and 326Q viruses exhibited an intermediate level of neuroinvasiveness (50% mortality within 50 days). The 326R and YF5.2iv viruses were not highly neuroinvasive, and the mortality percentages for the two viruses were not significantly different.

Sequence analysis of brain-associated viruses. To evaluate the possibility that the neuroinvasiveness of E326 mutant viruses resulted from reversions at either position 326 or other sites in the E protein, the nucleotide sequences of the prM-E region were analyzed for viruses recovered from brains of mice with encephalitis (Table 4). For two samples of the YF5.2iv control virus obtained on days 40 and 97 postinfection, no reversions were observed. One sample for the 326R virus obtained on day 85 contained no reversions. For the 326Q and 326S viruses, one and three samples, respectively, obtained between 21 and 23 days postinfection exhibited no reversions. For the 326A virus, two samples from days 16 and 17 contained no reversions and one sample obtained on day 71 contained only the neuroadaptive substitution 305V. For the 326D virus, three samples contained no reversions. For the 326G virus, two samples contained no reversions, whereas a third sample from day 160 contained two neuroadaptive substitutions (52G and 173T [previously observed in the parental SPYF-MN virus {3}]). Surprisingly, three samples of 326E obtained between days 10 and 16 postinfection contained the substitution 305S. Further evaluation of this observation was undertaken by review of the sequence data for the virus stock preparations used for the mouse experiments. The sequence of the parental virus stock prepared by plaque purification was confirmed to contain phenylalanine at position 305. However the amplified passage derived from this preparation in retrospect was found to contain a small percentage (<10%) of a single nucleotide substi-

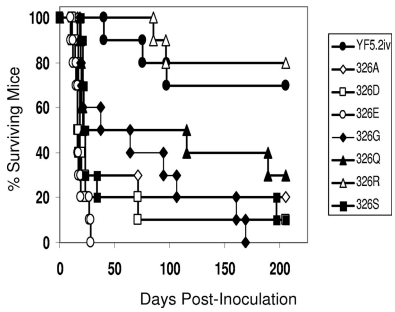

FIG. 3. Mortality data for SCID/ICR mice inoculated with viruses containing substitutions at position 326. The experimental procedures were carried out as described in Materials and Methods. Groups of 10 mice per virus were tested. The *P* values for mortality rates at 50 days were as follows, with a *P* value of <0.05 considered significant: 326E versus 326S or 326A, $P = 0.473$; 326E versus 326G, $P = 0.999$; 326E versus 326Q, $P = 0.210$; 326E versus YF5.2iv, $P = 0.003$; 326E versus 326R, $P = 0007$; 326Q versus YF5.2iv, $P = 0.178$; 326Q versus 326R, $P = 0.069$; 326Q versus 326A or 326S, $P = 0.999$; YF5.2iv versus 326R, $P = 0.999$. The average survival time data in days (mean ± standard deviation, median) were as follows: 326E, 17.7 ± 4.9, 16; 326D, 22.6 ± 18, 16; 326S, 23.7 ± 2.8, 25; 326A, 25 ± 17.9, 18; 326Q, 55.1 ± 63.6, 17; 326G, 69 ± 55.3, 52.5; 326R, 87.5 ± 2.5, 90; YF5.2iv, 66.6 ± 23.2, 75. *P* values (two sided) for comparison of the average survival times (log rank test), with a *P* value of <0.05 considered significant, were as follows: 326E versus 326D, 0.810; 326E versus 326Q, 307; 326E versus 326A, 0.167; 326E versus 326G, 0.103; 326E versus 326S, 0.026; 326D versus 326Q, 0.222; 326D versus 326A, 0.193; 326D versus 326G, 0.094; 326D versus 326G, 0.047; 326S versus 326Q, 0.645; 326S versus 326G, 0.502; 326S versus 326A, 0.002; 326A versus 326Q, 0.681; 326A versus 326G, 0.502; 326Q versus 326G, 0.880.

tution at nt 1887 (T to C), encoding a serine instead of phenylalanine. To confirm this observation, a second independent passage of the parental virus stock was prepared and was found to contain the same nucleotide substitution at approximately 30% of the predicted sequence. Thus, the 305S mutation observed in brain-associated virus from mice inoculated with 326E resulted from selection of a preexisting variant rather than from spontaneous mutation in vivo prior to or after neuroinvasion.

Heparin experiments. The attenuation of neuroinvasiveness associated with the 326K and 380T viruses suggested that a positive charge cluster involving these residues within domain III may be functionally important for this phenomenon (see the modeling data below). To investigate this question, a heparin-Sepharose plaque inhibition assay was used to determine if there was a correlation between heparin binding and neuroinvasiveness. The results are shown in Fig. 4A. Nonneuroadapted dengue 2 virus strain NGC was used as a positive control, since the heparin binding properties of this strain have been well characterized (6). Heparin-Sepharose inhibited plaque formation by dengue 2 virus by 85 to 88% in different experiments. YF5.2iv virus was also very sensitive to heparin-Sepharose inhibition of plaque formation in the range of 95 to 97%. The 305V virus was very similar to YF5.2iv virus in sensitivity to heparin. The 380T virus was less sensitive to heparin inhibition, with values in the range of 75 to 82%. The SPYF-H3 and 326E viruses were not highly sensitive to heparin-Sepharose, with only 35 to 45% and 45 to 58% inhibition, respectively, in different experiments. The differences between the SPYF-H3 and 326E viruses were not significant. The differences between either SPYF-H3 or 326E and YF5.2iv, 305V, and 380T viruses were all significant.

Results of heparin-Sepharose inhibition for viruses containing amino acid substitutions at position 326 are shown in Fig. 4B. YF5.2iv virus was inhibited to a level of 85 to 95%. 326R exhibited a similar level of sensitivity. The remainder of the viruses were all significantly different from YF5.2iv and 326R in sensitivity, with inhibition of plaque formation in the range of 38 to 65%. 326D exhibited the lowest level of sensitivity.

Based on the observation that YF5.2iv virus was highly sensitive to heparin-Sepharose, the amino acid sequence of the E protein was scanned for heparin binding motifs using the linear binding sequence XBBXBX, XBBBXXBX, or TXXBXXTBX XXTBB (12). This revealed no exact sequence matches with the motif, suggesting that the heparin binding site is not based simply on the linear sequence of domain III.

Modeling of virulence loci. The homology model for YFV domain III, based on the WNV E protein, was used to gain insight into the effects of the SPYF-specific amino acid substitutions and of the substitutions at position 326 on the properties of domain III. WNV structures 1s6nA (domain III) and 2169A (E protein) were used for modeling, as described in Materials and Methods and as shown in Fig. 5. Use of these two WNV structures as templates gave somewhat different results with respect to mapping of electrostatic potentials in domain III of the YFV E protein. The WNV 1s6nA structure was used as a model to reconcile the data from heparin binding experiments with the data from neuroinvasiveness testing, since no substitutions outside of domain III of the YFV E protein were involved in the analysis.

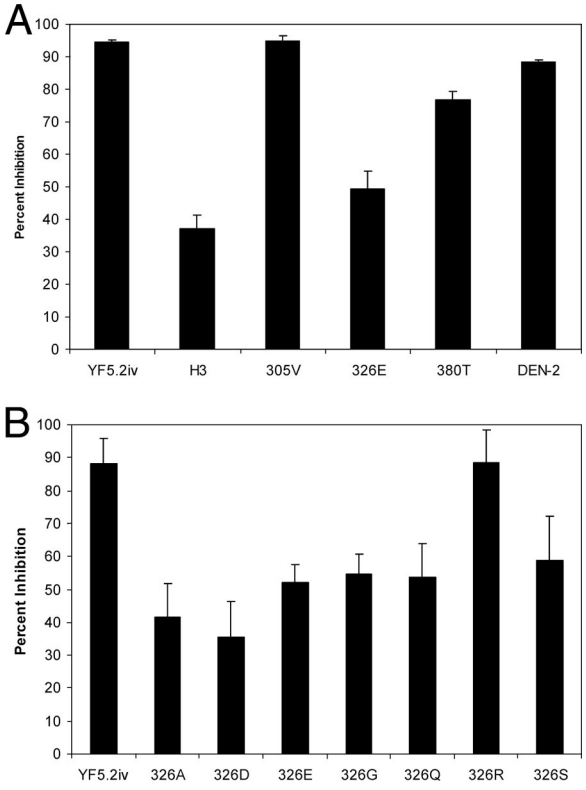

FIG. 4. Heparin inhibition of YFV plaque formation. The values represent means plus standard deviations. (A) SPYF-specific substitutions in domain III. The results represent data from four independent experiments. Statistical values for differences in heparin inhibition were as follows (P values of <0.05 were considered significant): YF5.2iv versus SPYF-H3, 326E, 380T, or DEN-2 (dengue 2 virus), $P < 0.0001$; YF5.2iv versus 305V, $P = 0.815$; 305V versus 380T, $P = 0.001$; 305V versus 326E or SPYF-H3, $P < 0.001$; 305V versus DEN-2, $P = 0.004$; 380T versus SPYF-H3, $P < 0.001$; 380T versus 326E, $P = 0.002$; 380T versus DEN-2, $P = 0.002$; SPYF-H3 versus 326E, $P = 0.117$; SPYF-H3 versus DEN-2, $P < 0.001$; 326E versus DEN-2, $P < 0.001$. (B) Viruses containing substitutions at position 326. The results represent data from six independent experiments. Statistical values for differences in heparin inhibition were as follows (P values of <0.05 were considered significant): YF5.2iv versus 326A, 326G, 326D, 326Q, 326S, or 326E, $P < 0.0001$; YF5.2iv versus 326R, $P = 0.964$; 326E versus 326R, $P < 0.0001$; 326E versus 326D, $P = 0.007$; 326E versus 326G, $P = 0.470$; 326E versus 326A, $P = 0.046$; 326E versus 326S, $P = 0.30$; 326E versus 326Q, $P = 0.766$; 326D versus 326R, $P < 0.0001$; 326D versus 326G, $P = 0.003$; 326D versus 326A, $P = 0.336$; 326D versus 326S, $P = 0.008$; 326D versus 326Q, $P = 0.013$; 326A versus 326R, $P < 0.0001$; 326A versus 326G, $P = 0.021$; 326A versus 326S, $P = 0.032$; 326A versus 326Q, $P = 0.065$; 326G versus 326Q, $P = 0.828$; 326G versus 326S, $P = 0.526$; 326Q versus 326S, $P = 0.480$; 326Q versus 326R, $P < 0.0001$.

According to the model, the neuroadaptive determinants at positions 305, 326, and 380 of the YFV E protein occur on the upper half of domain III, with 326 lying above 380 (Fig. 5A and B). 305 lies within a pocket separating these two residues. In YF5.2iv, the lysine residue at 326 and the arginine residue at 380 contribute to a charge cluster that is located in the upper half of the domain adjacent to the surface contacting domain I (Fig. 5A). The model predicts an orientation of the lysine residue at position 326 that projects from the apical surface of the domain and forms an electrostatic interaction with an as-

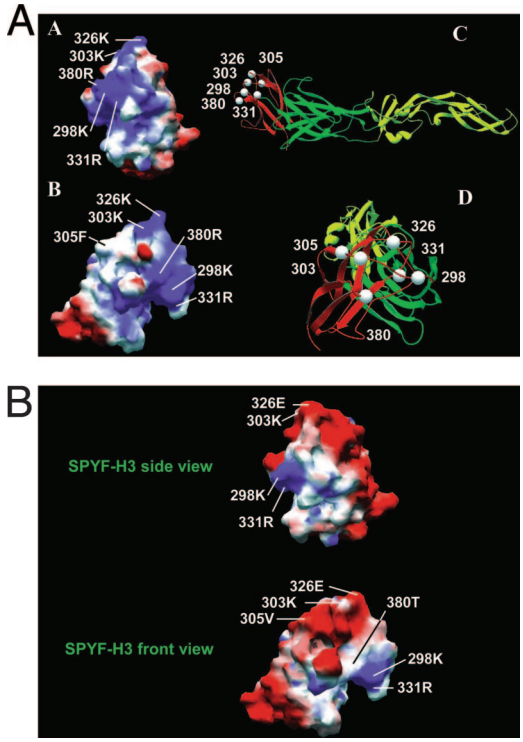

FIG. 5. (A) Homology model of the space-filling and electrostatic-potential maps for domain III of the YF5.2iv virus E protein (models A and B) based on the WNV structure. Model B is rotated clockwise to visualize residue 305F. Blue and red shading display regions of positive and negative charge, respectively. Models C and D are the ribbon diagrams for the E protein to show the orientations of domain III. Domains I, II, and III are shown in green, yellow, and red, respectively. (B) Model for domain III of the SPYF-H3 virus.

partic acid residue at position 360 (not shown). The charge cluster also involves the adjacent residues 303K, 298K, and 331R, which lie along the medial border of the domain. For YF5.2iv, the positive electrostatic potential generated by these five residues presumably accounts for the heparin binding activity that correlates with the attenuation of neuroinvasiveness observed in SCID mice.

Predicted effects of the neuroadaptive substitutions 305V, 326E, and 380T are shown in Fig. 5B. Substitution of valine at position 305 had no noticeable effect on the charge distribution in domain III. Introduction of a glutamic acid residue at position 326 markedly reduced the extent of the positive charge cluster. Substitution with threonine at position 380 reduced the charge distribution in the vicinity of residue 303. The combination of 326E and 380T, as occurs in the case of the SPYF-H3 virus, eliminated almost all of the charge cluster, except for some residual effects contributed by E298K and E331R.

The predicted effects of amino acid substitutions at position 326 are illustrated in Fig. 6. For the YF5.2iv and the 326R viruses, the positive charge cluster on the apical surface of domain III appeared very similar. For the 326D substitution, loss of the positive charge cluster across the upper surface of the domain and the surrounding lateral region was very similar to that shown for 326E. For the 326Q, 326S, 326A, and 326G substitutions, there was loss of most of the apical charge cluster

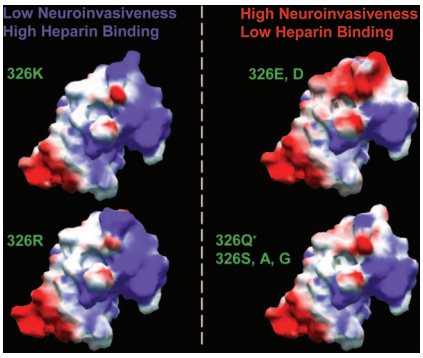

FIG. 6. Model of amino acid substitutions at position 326 in domain III of the YF5.2iv E protein. (Left) Structure of YF5.2iv (top) and the 326R substitution (bottom). (Right, top) Structure of 326E or 326D (the 326E model is shown, as the models for D and E substitutions are very similar). (Right, bottom) Model for 326G, 326Q, 326S, or 326A. The model for 326Q is shown, as it is representative of the models for the other substitutions, with slightly smaller neutral space filling at position 326 for side chain residues other than Q (data not shown).

with retention of only limited positive charge in the region of the lysine residue at position 303.

DISCUSSION

Neuroadaptation of virus strain YF17D caused by serial passages in mouse brain results in enhanced neurovirulence relative to nonneuroadapted virus, characterized by increased mortality rates, reduced average survival times, and a higher virus burden in the brain (3, 29, 33). As shown with a molecular clone of neuroadapted virus strain 17D (SPYF-MN), the genetic changes that accompany this neuroadaptation include multiple nucleotide substitutions throughout the structural, nonstructural, and 3′-untranslated regions of the viral genome (3). However, substitutions in the E protein are believed to be critical for the enhancement of virulence properties. Neuroadaptation has also been shown to enhance the neuroinvasiveness of YFV in SCID mice, suggesting that common molecular determinants in the E protein may be involved in the pathogenesis of disease in both the central nervous system and the periphery (3, 29). The results of the current experiments confirm that for YFV, a region within domain III of the E protein governs neuroinvasiveness as assessed in the SCID mouse model. This contrasts with other studies that have implicated molecular determinants within domains I, II, and III, as well as the stem-anchor region of the E protein, in the virulence of flaviviruses (1, 11, 19, 20, 27, 28, 30, 31, 32, 35).

Within domain III of the SPYF-MN E protein, substitutions 305F→V, 326K→E, and 380R→T were evaluated as the critical determinants of neuroinvasion in the SCID mouse model (29). Experiments with viruses containing these single substitutions revealed that 326E was necessary for high neuroinvasiveness. In contrast, neither 305V nor 380T by itself conferred such an effect. However it remains possible that the combination of these two substitutions without 326E could result in high neuroinvasiveness. Data to address this question are not currently available. However, if there were subdominant effects of 305V and 380T, a difference in the neuroinvasiveness of

SPYF-H3 and 326E viruses over a range of doses might be expected. Experiments that compared these two viruses at doses from approximately 2 to 5.5 log PFU did not reveal any major quantitative difference in neuroinvasiveness. These results also support the conclusion that 326E is a critical determinant of neuroinvasiveness in the SCID mouse model.

Testing of a panel of viruses containing various amino acid substitutions at position 326 in the E protein revealed that attenuation of neuroinvasiveness resulted from the presence of a positive-charge residue, either lysine or arginine, at this position. All other amino acid substitutions conferred increased neuroinvasiveness, based on day 50 mortality. 326E, 326D, 326A, and 326S yielded viruses with high neuroinvasiveness, whereas 326G and 326Q yielded viruses with an intermediate level of neuroinvasiveness. Thus, there is no obligatory requirement for the 326E substitution to confer a neuroinvasive phenotype, although a negative-charge substitution of either aspartic acid or glutamic acid did confer the highest level of virulence. Although neurovirulence was not tested for the panel of 326 mutant viruses, YF5.2iv virus has been shown to be highly neurovirulent in SCID mice (3). Given that all 326 mutant viruses except 326R exhibited greater virulence than YF5.2iv, it is likely that potential differences in neurovirulence do not contribute to the results observed here for neuroinvasiveness.

Although the method of quantitation of virus doses was based on plaque assay rather than mouse infectivity and differences in heparin binding activity may have introduced some discrepancy in the effective doses when comparing YF5.2iv with 326E, the large differences in mortality rates and survival times between these viruses and the preservation of the difference over a dose range up to 3.0 log PFU (Table 3) suggests that a dose discrepancy is not likely to explain the observed differences in neuroinvasiveness.

Sequencing of viruses recovered from the brains of the mice confirmed that the high neuroinvasiveness observed with substitutions at position 326 did not result from reversions at that position. However, for the 326E virus, sequencing of brain-associated viruses from mice that developed encephalitis consistently revealed the second-site substitution of serine for phenylalanine at position 305. This reversion occurred at the level of cell culture passage of the 326E virus and then underwent selection during replication in SCID mice. 325S is found in the virulent YFV strains Asibi, FVV, and FNV, but its role in either neurotropism or viscerotropism is undefined. We cannot exclude at present the possibility that 305S contributes in some manner as a virulence determinant in association with 326E. In an interferon-deficient mouse model of neuroinvasiveness, 325S did not appear to increase the virulence of YFV 17D. It is notable that in the SCID mouse model, neither the 326D virus nor any of the other viruses exhibiting neuroinvasiveness could be associated with reversion at position 325, indicating that the presence of a negative charge alone at position 326 may not drive this selection. Substitutions at position 305 (phenylalanine, serine, or valine) have also been observed in the context of neutralization-escape mutants of YF17D virus that involve replacement of proline at position 325 with either leucine or serine (32). The molecular basis for this covariation of substitutions involving positions 305 and 325/326 remains to be defined. Mutations at 305 may compensate in some manner

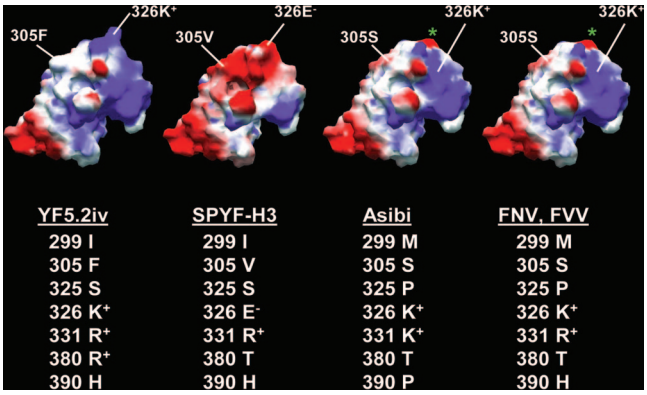

FIG. 7. Model of domain III for the YF5.2iv and SPYF-H3 viruses in comparison to those for the Asibi, FNV, and FVV strains of YFV. The models show the positions of residue E326. 326K and E326E are at the apex of the domain for YF5.2iv and SPYF-H3, respectively; 326K is folded downward and medially for Asibi, FNV, and FVV. The green asterisk indicates the position of 360D, which is predicted to interact with 326K for YF5.2iv, but not for Asibi, FNV, or FVV. The amino acid sequences of domain III for the viruses are shown at the bottom. The sequences for FNV and FVV are identical.

for the effects of 325/326 substitutions on the E protein. Modeling of these substitutions in domain III of the YFV E protein did not reveal any explanation for this phenomenon (data not shown).

In the case of the 326A and 326G viruses, mortality observed after 50 days was associated with reversions. The reversions included 305F→V, 173I→T, and 52R→G, all of which are known to result from neuroadaptation (32), even though they have not been validated as determinants of increased neuroinvasiveness in SCID mice (29). The significance of these reversions remains to be defined. They may reflect adaptation to growth in mouse tissue without representing critical virulence determinants (see below).

The current experiments also revealed that lysine and arginine at positions 326 and 380 contribute to a heparin binding activity associated with domain III of the YFV E protein. The infectivity of YF17D virus for cells in culture has been reported to be sensitive to inhibition by heparin, although no heparin binding motifs on the E protein have been characterized (10). The lack of an identifiable linear heparin binding motif suggests that formation of a binding site may involve residues in adjacent loops in the region of residues 326K and 380T and possibly other charged residues on the upper lateral surface of the domain, such as 303K and 298K. Modeling of the electrostatic charge in this region of the YFV E protein predicts an extended region of positive charge contributed by these residues collectively (Fig. 5A and B). For the 303 position, preliminary data also indicate that amino acid substitutions other than lysine increase the neuroinvasiveness of YF5.2iv virus. In particular, 303Q, which is associated with neurovirulence reversion of YF17D vaccine in humans (13), appears to be a virulence determinant in the SCID mouse model (T. J. Chambers and J. Nickells, unpublished data).

At present, the exact relationship between the heparin sensitivity of the YFV E protein and neuroinvasiveness is unclear. For instance, the 380T substitution significantly reduced heparin sensitivity but does not appear to be critical for neuroin-

vasiveness, indicating that loss of heparin sensitivity alone is insufficient to drive neuroinvasiveness. In this regard, even though the 326E substitution greatly diminishes heparin sensitivity, it may have additional effects on activities of the E protein that affect neuroinvasion, such as receptor binding or postreceptor events involved in virus entry. Such effects may act in concert with reduced GAG binding to result in a highly neuroinvasive phenotype for viruses that contain 326E.

Derivation of YF17D virus from its virulent progenitor Asibi strain by passage in tissue of chicken embryo origin may mimic the phenomenon of cell culture selection for heparin binding variants of Murray Valley encephalitis, Japanese encephalitis, dengue, and tick-borne encephalitis viruses (14, 15, 16, 21). As a result, the mechanism of attenuation of YFV virulence might be related to the acquisition of heparin binding activity, and the observed effects of the 326K substitution on the virulence of SPYF-MN virus may reflect a broader phenomenon relative to the properties of other virulent YFV strains, such as Asibi, FNV, and FVV viruses. Sequence comparisons and modeling of domain III for these virus strains revealed that they contain a lysine residue at position 326, but the predicted electrostatic potentials do not resemble that of YF5.2iv (Fig. 7). This is due in part to a substitution of threonine for arginine at position 380. However, a proline residue at position 325 (instead of serine, as in YF5.2iv and SPYF-MN) may be responsible for altering the local structure to prevent an orientation of the lysine at position 326 as observed in the YF5.2iv E protein. The interaction with 360D, as predicted for the YF5.2iv model, is also disrupted. These observations suggest that a glutamic acid at position 326 in the SPYF-MN virus and a proline at position 325 in Asibi, FNV, and FVV viruses may cause the same effect in terms of reducing a heparin binding activity that is involved in attenuation of virulence. If that is the case, then domain III may contribute primarily as a modulator of YFV virulence, with determinants of different tropisms located elsewhere in the E protein or other regions of the viral genome.

In previous studies, the high neuroinvasiveness of the SPYF-H3 virus for SCID mice was associated with systemic infection characterized by viremia, low to moderate virus burdens in peripheral organs, and high virus titers in the brain (29). The 326E virus differs from this pattern in that systemic infection was less frequent and virus was found predominantly at the site of inoculation (the peritoneal cavity). While the 326E virus clearly exhibits neuroinvasiveness for SCID mice, the restricted capacity to cause the disseminated infection typical of the SPYF-H3 virus may result from differences between these viruses at positions 305 and 380. For instance, these residues may not be critical for neuroinvasion but may represent adaptive mutations that contribute to increased virus burdens in peripheral tissues. 326E virus was moderately impaired for virus production in BHK cells, which may also reflect a lack of efficient virus spread in rodent tissue. The appearance of the revertant mutation 305F→V in brain-associated virus recovered from SCID mice inoculated with 326A virus (Table 5) is consistent with this hypothesis, although further studies are needed to verify that the mutation facilitates virus growth in peripheral tissues. As noted earlier, the greater heparin binding activity of YF5.2iv virus than of 326E and SPYF-H3 may have created a discrepancy in measuring tissue virus titers in these experiments. Since this effect would be expected to increase the relative yields of YF5.2iv virus, and because very low levels of YF5.2iv virus were observed in the tissues, the impact of this factor on the conclusions is judged to be minor.

TABLE 5. Revertant mutations of E326 viruses[a]

Virus	Day[b]	Nucleotide change	Amino acid change
326K(YF5.2iv)	40	No change	No change
	97	No change	No change
326R	85	No change	No change
326Q	21	No change	No change
326G	37	No change	No change
	64	499 (A to G)	Silent
		1705 (A to G)	Silent
	160	649 (G to A)	Silent
		1127 (A to G)	E52 (R to G)
		1491 (T to C)	E173 (I to T)
		1645 (G to A)	Silent
326A	16	2401 (C/T)[c]	Silent
	17	No change	No change
	17	No change	No change
	71	1886 (T to G)	E305 (F to V)
326S	21	No change	No change
	22	No change	No change
	23	No change	No change
326D	16	No change	No change
	16	No change	No change
	17	No change	No change
	71	895 (C/T)[c]	Silent
326E	10	1887 (T to C)	E305 (F to S)
	15	1887 (T to C)	E305 (F to S)
	16	1887 (T to C)	E305 (F to S)

[a] Sequence data on viruses recovered from mouse brains.
[b] Day indicates day postinfection.
[c] A doublet was observed at these positions.

There is limited understanding of the molecular basis for neurovirulence of the YF17D vaccine in humans and the syndrome of vaccine-associated encephalitis (9). The available data suggest that reversions involving one or two mutations in the E protein are involved (13). Data from the current studies support this hypothesis, since the 326E substitution can cause YF17D to revert to a highly neuroinvasive virus in the mouse model. However, we acknowledge that differences between the pathogeneses of neurotropic disease in mice and humans do not allow any definite conclusions regarding the molecular basis for YF17D-associated encephalitis in humans. It is possible that multiple pathways, involving other mutations in the E protein or other regions of the viral genome, may also exist for reversion of YF17D vaccine to a virulent phenotype in humans. We also observe that, as for other flaviviruses and as observed for YFV in the interferon-deficient mouse model (17), there is a correlation between heparin binding activity involving domain III of the YFV E protein and attenuation of neuroinvasiveness. We propose that this activity may apply broadly as a mechanism of attenuation of YFV virulence.

ACKNOWLEDGMENT

This work was supported by a grant from the CDC (CI-000094).

REFERENCES

1. **Allison, S. L., K. Stiasny, K. Stadler, C. W. Mandl, and F. X. Heinz.** 1999. Mapping of functional elements in the stem-anchor region of tick-borne encephalitis virus envelope protein E. J. Virol. **73:**5605–5612.
2. **Barrett, A. D. T., and E. A. Gould.** 1986. Comparison of neurovirulence of different strains of yellow fever virus in mice. J. Gen. Virol. **67:**631–637.

3. **Chambers, T. J., and M. Nickells.** 2001. Neuroadapted yellow fever virus 17D: genetic and biological characterization of a highly mouse-neurovirulent virus and its infectious molecular clone. J. Virol. **75:**10912–10922.
4. **Chambers, T. J., and M. S. Diamond.** 2003. Pathogenesis of flavivirus encephalitis. Adv. Virus Res. **60:**273–342.
5. **Chambers, T. J., Y. Liang, D. A. Droll, J. J. Schlesinger, A. Davidson, P. J. Wright, and X. Jiang.** 2003. Yellow fever/dengue-2 and dengue-4 chimeric viruses: biological properties, immunogenicity, and protection against dengue encephalitis in the mouse model. J. Virol. **77:**3655–3668.
6. **Chen, Y., T. Maguire, R. E. Hileman, J. R. Fromm, J. D. Esko, R. J. Linhardt, and R. M. Marks.** 1997. Dengue virus infectivity depends on envelope protein binding to target cell heparan sulfate. Nat. Med. **3:**866–871.
7. **Collier, W. A., H. De Roever-Bonnet, and J. Hoekstra.** 1959. A neurotropic variety of the vaccine strain 17D. Trop. Geogr. Med. **11:**80.
8. **Fitzgeorge, R., and C. J. Bradish.** 1980. The in vivo differentiation of strains of yellow fever virus in mice. J. Gen. Virol. **46:**1–13.
9. **Freestone, D. S.** 1994. Yellow fever vaccine, p. 741–779. *In* S. A. Plotkin and E. M. Mortimer (ed.), Vaccines, 2nd ed. W. B. Saunders, Philadelphia, PA.
10. **Germi, R., J.-M. Crance, D. Garin, J. Guimet, H. Lortat-Jacob, R. W. H. Ruigrok, J.-P. Zarski, and E. Drouet.** 2002. Heparan sulfate-mediated binding of infectious dengue virus type 2 and yellow fever virus. Virology **292:** 162–168.
11. **Hasegawa, H., M. Yoshida, T. Shiosaka, S. Fujita, and Y. Kobayashi.** 1992. Mutations in the envelope protein of Japanese encephalitis virus affect entry into cultured cells and virulence in mice. Virology **191:**158–165.
12. **Hileman, R. E., J. R. Fromm, J. M. Weiler, and R. J. Linhardt.** 1998. Glycosaminoglycan-protein interactions: definition of consensus sites in glycosaminoglycan binding proteins. BioEssays **20:**156–167.
13. **Jennings, A. D., C. A. Gibson, B. R. Miller, J. H. Mathews, C. J. Mitchell, J. T. Roehrig, D. J. Wood, F. Taffs, B. K. Sil, S. N. Whitby, et al.** 1994. Analysis of a yellow fever virus isolated from a fatal case of vaccine-associated encephalitis. J. Infect. Dis. **169:**512–518.
14. **Lee, E., and M. Lobigs.** 2002. Mechanism of virulence attenuation of glycosaminoglycan-binding variants of Japanese encephalitis virus and Murray Valley encephalitis virus. J. Virol. **76:**4901–4911.
15. **Lee, E., R. A. Hall, and M. Lobigs.** 2004. Common E protein determinants for attenuation of glycosaminoglycan-binding variants of Japanese encephalitis and West Nile viruses. J. Virol. **78:**8271–8280.
16. **Lee, E., P. J. Wright, A. Davidson, and M. Lobigs.** 2006. Virulence attenuation of dengue virus due to augmented glycosaminoglycan binding affinity and restriction in extraneural dissemination. J. Gen. Virol. **87:**2791–2801.
17. **Lee, E., and M. Lobigs.** 2008. E protein domain III determinants of yellow fever virus 17D vaccine strain enhance binding to glycosaminoglycans, impede virus spread, and attenuate virulence. J. Virol. **82:**6024–6033.
18. **Liprandi, F.** 1981. Isolation of plaque variants differing in virulence from the 17D strain of yellow fever virus. J. Virol. **56:**363–370.
19. **Lobigs, M., R. Usha, A. Nestorowicz, I. D. Marshall, R. C. Weir, and L. Dalgarno.** 1990. Host cell selection of Murray Valley encephalitis virus variants altered at an RGD sequence in the envelope protein and in mouse virulence. Virology **176:**587–595.
20. **Mandl, C. W., S. L. Allison, H. Holzmann, T. Meixner, and F. X. Heinz.** 2000. Attenuation of tick-borne encephalitis virus by structure-based site-specific mutagenesis of a putative flavivirus receptor binding site. J. Virol. **74:**9601–9609.
21. **Mandl, C. W., H. Kroschewski, S. L. Allison, R. Kofler, H. Holzmann, T. Meixner, and F. X. Heinz.** 2001. Adaptation of tick-borne encephalitis virus to BHK-21 cells results in the formation of multiple heparan sulfate binding sites in the envelope protein and attenuation in vivo. J. Virol. **75:**5627–5637.
22. **McMinn, P. C., E. Lee, S. Hartley, J. T. Roehrig, L. Dalgarno, and R. C. Weir.** 1995. Murray Valley encephalitis virus envelope protein antigenic variants with altered hemagglutination properties and reduced neuroinvasiveness in mice. Virology **211:**10–20.
23. **McMinn, P. C., R. C. Weir, and L. Dalgarno.** 1996. A mouse-attenuated envelope protein variant of Murray Valley encephalitis virus with altered fusion activity. J. Gen. Virol. **77:**2085–2088.
24. **McMinn, P. C.** 1997. The molecular basis of virulence of the encephalitogenic flaviviruses. J. Gen. Virol. **78:**2711–2722.
25. **Meers, P. D.** 1959. Adaptation of the 17D yellow fever virus to mouse brain by serial passage. Trans. R. Soc. Trop. Med. Hyg. **53:**445–457.
26. **Monath, T. P.** 1986. Pathobiology of the flaviviruses, p. 375–440. *In* S. Schlesinger and M. J. Schlesinger (ed.), The Togaviridae and the Flaviviridae. Plenum Press, New York, NY.
27. **Ni, H., and A. D. T. Barrett.** 1998. Attenuation of Japanese encephalitis virus by selection of its mouse brain membrane receptor preparation escape mutants. Virology **241:**30–36.
28. **Ni, H., K. D. Ryman, H. Wang, M. F. Saeed, R. Hull, D. Wood, P. D. Minor, S. J. Watowich, and A. D. T. Barrett.** 2000. Interaction of yellow fever virus French neurotropic vaccine strain with monkey brain: characterization of monkey brain membrane receptor escape variants. J. Virol. **74:**2903–2906.
29. **Nickells, M., and T. J. Chambers.** 2003. Neuroadapted yellow fever virus 17D. Determinants in the envelope protein govern neuroinvasiveness for SCID mice. J. Virol. **77:**12232–12242.
30. **Rice, C. M., A. Grakoui, R. Galler, and T. J. Chambers.** 1989. Transcription of infectious yellow fever virus RNA from full-length cDNA templates produced by in vitro ligation. New Biol. **1:**285–296.
31. **Ryman, K. D., H. Xie, T. N. Ledger, G. A. Campbell, and A. D. T. Barrett.** 1997. Antigenic variants of yellow fever virus with an altered neurovirulence phenotype in mice. Virology **230:**376–380.
32. **Ryman, K. D., T. N. Ledger, G. A. Campbell, S. J. Watowich, and A. D. T. Barrett.** 1998. Mutation in a 17D-204 vaccine substrain-specific envelope protein epitope alters the pathogenesis of yellow fever virus in mice. Virology **244:**59–65.
33. **Schlesinger, J. J., S. Chapman, A. Nestorowicz, C. M. Rice, T. E. Ginocchio, and T. J. Chambers.** 1996. Replication of yellow fever virus in the mouse central nervous system: comparison of neuroadapted and nonneuroadapted virus and partial sequence analysis of the neuroadapted strain. J. Gen. Virol. **77:**1277–1285.
34. **Schlesinger, R. W.** 1980. Virus-host interactions in natural and experimental infections with alphaviruses and flaviviruses, p. 83–104. *In* R. W. Schlesinger (ed.), The togaviruses. Academic Press, New York, NY.
35. **Stiasny, K., S. L. Allison, A. Marchler-Bauer, C. Kunz, and F. X. Heinz.** 1996. Structural requirements for low-pH-induced rearrangements in the envelope glycoprotein of tick-borne encephalitis virus. J. Virol. **70:**8142–8147.
36. **Theiler, M.** 1951. The virus, p. 46–136. *In* G. K. Strode (ed.), Yellow fever. McGraw-Hill, New York, NY.
37. **Vlaycheva, L. A., and T. J. Chambers.** 2002. Neuroblastoma cell-adapted yellow fever 17D virus: characterization of a viral variant associated with persistent infection and decreased virus spread. J. Virol. **76:**6172–6184.